INTERNATIONAL JOURNAL FOR NUMERICAL METHODS IN FLUIDS, VOL. 16, 421–443 (1993)

DEVELOPMENT OF A HYBRID k–ε TURBULENCE MODEL FOR SWIRLING RECIRCULATING FLOWS UNDER MODERATE TO STRONG SWIRL INTENSITIES

KEH-CHIN CHANG* AND CHING-SHUN CHEN†

Institute of Aeronautics and Astronautics, National Cheng-Kung University, Tainan, Taiwan, R.O.C.

SUMMARY

A hybrid k–ε turbulence model, based on the concept that the modification of anisotropic effects should not be made in the flow regions inherent to small streamline curvatures, has been developed and examined with the swirling recirculating flows, with the swirl levels ranging from 0·6 to 1·23 in abrupt pipe expansion. A fairly satisfactory agreement of model predictions with the experimental data shows that this hybrid k–ε model can perform better simulation of swirling recirculating flows as compared to the standard k–ε model and the modified k–ε model proposed by Abujelala and Lilley.

KEY WORDS Turbulence Swirling recirculating flow

1. INTRODUCTION

Swirl flows have been applied in a very wild range of engineering practices. Extensive review on the phenomena and application of swirl flows has been made by Lilley,[1] Gupta *et al.*,[2] as well as Sloan *et al.*[3] and will not be repeated here. Swirling motion is the result of an impartation of a tangential (or azimuthal) velocity component by use of a swirl generator positioned upstream of the flow field. The profiles of tangential velocity component in some cross-section of the swirl flows can be considered as a composition of forced-vortex (rigid-body rotation) flow and free-vortex (potential-vortex) flow (see Figure 1 of Reference 3). The turbulence characteristics of the swirl flows between the central forced-vortex region and the surrounding free-vortex region are obviously different. The forced-vortex region extends its boundary to the location of maximum tangential velocity, with the rigid-body rotation flow being 'shear'- or 'strain'-free, but not vorticity-free. However, the free-vortex region can be considered as being irrotational or vorticity-free.[3] Swirls with sufficient strength (larger than the critical swirl number) possess sufficient radial and axial pressure gradients to form a Central Toroidal Recirculation Zone (CTRZ), which is not observed at weaker degrees of swirl. In this study, the degree of swirl will be characterized by the swirl number S, which is a non-dimensional number representing axial flux of swirl momentum divided by axial flux of axial momentum times the equivalent nozzle radius

* Associate Professor
† Graduate Student

0271–2091/93/050421–23$16.50

Received May 1992
Revised November 1992

and is given by

$$S=\frac{1}{R}\frac{\int_0^R r^2uw\,\mathrm{d}r}{\int_0^R ru^2\,\mathrm{d}r}, \tag{1}$$

where R is the inner duct radius.

In combustion system, high swirling flows have been commonly utilized to improve the flame stability through the formation of central toroidal recirculation zones and to reduce the length of combustors by virtue of fast mixing and high entrainment rates of the ambient fluid. For some high-performance combustors such as that of ramjet engine, gas turbine, etc., the CTRZ is usually accompanied by the Corner Recirculation Zone (CRZ), that is provoked by the sudden expansion in flow field, to help reach the aforementioned goal. In this work, we focus our attention on the turbulent flows with strong swirl intensities in abrupt pipe expansion (as demonstrated in Figure 1), i.e. the swirling recirculating flows.

In principle, there is no need to adopt special practices for turbulent flow, for the Navier–Stokes equations apply equally to a turbulent flow as to a laminar one. However, although the advent of the supercomputer permits Direct Numerical Simulation (DNS) of turbulent motion in simple geometry, this is not a practically passable route for engineering application of today yet. Instead, the time-averaged decompositions are commonly used for the conservation equations of turbulent flows, but there is no direct way to estimate the magnitudes of statistical correlations in the averaged equations. The well-known turbulence closure problem occurs in order to supply the information missing from the averaged equations.

Based on the consideration of applicability, accuracy, simplicity and economy of computer efforts, quite a few turbulence-models-associated phenomenological conjectures have been proposed for the simulation of turbulent flows. These models have been described in several excellent review papers, for instance, Reference 4. Among these models, one successful two-equation model, the standard (original) k–ε turbulence model, has been widely applied to engineering practice, but has been criticized as being only qualitatively correct in the simulation of confined swirling flows.[3–9] The deficiency of the standard k–ε model stems perhaps from the neglect of anisotropic viscosity and additional turbulence generation arising from the effects of streamline curvature.[4,10] The simplest modification to the standard k–ε model that was based on adjustment of

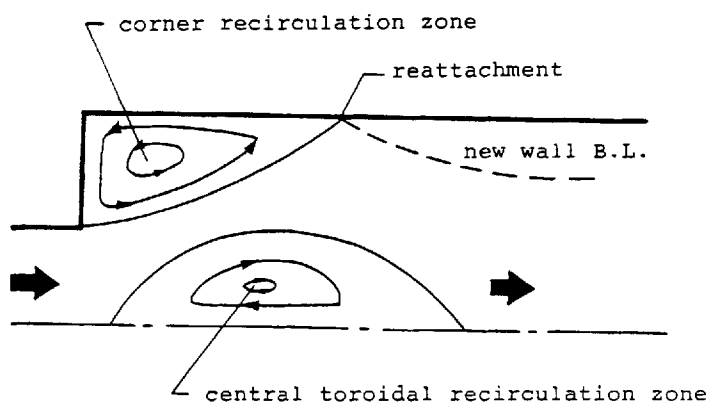

Figure 1. Flow characteristics in an abrupt pipe expansion with high swirl numbers

three empirical constants in the model[11] was not found to be capable of predicting accurately the swirling recirculating flow fields in a wide range of swirl number.[12] Many other *ad hoc* modifications to the standard k–ε model, taking into account the enhanced turbulence diffusion caused by the extra strain rates incorporated with streamline curvature, have been proposed.[3,4,13] However, none of the existing modified k–ε models were reported to be able to yield satisfactory predictions of swirling flows with the swirl intensities ranging from low to high extents.[3,5,6,13]

An attractive alternative is the use of higher-order turbulence closure models such as the Algebraic Stress Models (ASM) and the Reynolds Stress Models (RSM). Many studies[3–5,14] reported that, in swirling recirculating flows, the improvements of flow field predictions using the ASM were not so pronounced in comparison with those using the k–ε models. Nikjooy and Mongia[15] found that the ASM was unsuitable for prediction of the CTRZ when applying to swirling recirulating flows. Fu *et al.*[16] pointed out further that the ASM hypothesis seriously misrepresented the diffusive transport of the stress components and this defeat was aggravated by a failure accounting for additive swirl-related stress transport terms in the algebraic modelling process. For the highly anisotropic flows such as the swirling recirculating case, the RSM has been demonstrated to be capable of reproducing, to a certain extent, the major features of the flows,[15–18] but it greatly increased the computational complexity and time requirement. Furthermore, the fact remains that as the order of the turbulence model is increased, the number of empirical constants increases, and insufficient model assessments lead to less generality of these empirical constants in applications.[15]

From the viewpoint of an engineer, a general method for flow predictions must comprise both a physical model which reflects the true nature of the flow and an efficient mathematical apparatus which permits accurate and yet economical calculations. It is, so far, not clear whether the higher-order models are more valuable than the k–ε model. Moreover, in our previous work,[19] a hybrid k–ε model, which was based on an idea that modification of anisotropic effects should not be made in the regions where the streamline curvature was small, has been successfully developed for the case of recirculating flows without swirling motion. The success of the previous work leads to the present attempt, that is, developing a hybrid modification to the k–ε turbulence model for the simulation of swirling recirculating flows.

2. MODIFICATION OF ANISOTROPIC EFFECTS TO k–ε MODEL

In the k–ε turbulence model, the turbulent kinetic energy (k) and its dissipation rate (ε) are estimated from their corresponding transport equations to relate the Reynolds stress and the rate of strain. In addition, the standard k–ε model describes the turbulence characteristics at any point in the flow field by a single length scale which is determined by the hypothesis of isotropic turbulence structure. An extensive experimental investigation[10] reveals that the turbulence structures near the recirculation zone and swirl zone are sometimes quite anisotropic. This inference stems from an observation that the extra rates are imposed on the strong recirculation or swirl zone and this would tend to increase both the velocity and the length scale of turbulence. When significant streamline curvatures are introduced into this kind of flow field, the standard k–ε model cannot adequately account for the enhanced turbulence diffusion caused by the extra strain rates associated with streamline curvature. To remedy this deficiency, some argued that the inappropriateness of the k–ε model to the swirling recirculating flows might be mainly stemming from the ε equation.[1–3] In general, the source term of the ε equation can be modified, accounting for the anisotropic effects, in many ways.[3,5,13] One popular way is to express the empirical constant C_2 of the ε equation (see Table I) as a function of the swirling and curvature Richardson numbers, which are the measures of the extra strain rates due to swirling and recirculating

Table I. Governing equations

$$\frac{\partial}{\partial x}(\rho u\phi)+\frac{1}{r}\frac{\partial}{\partial r}(r\rho v\phi)-\frac{\partial}{\partial x}\left(\Gamma_\phi\frac{\partial\phi}{\partial x}\right)-\frac{1}{r}\frac{\partial}{\partial r}\left(r\Gamma_\phi\frac{\partial\phi}{\partial r}\right)=S_\phi$$

ϕ	Γ_ϕ	S_ϕ
u	μ_{eff}	$\frac{\partial}{\partial x}\left(\mu_{\text{eff}}\frac{\partial u}{\partial x}\right)+\frac{1}{r}\frac{\partial}{\partial r}\left(r\mu_{\text{eff}}\frac{\partial v}{\partial x}\right)-\frac{\partial p}{\partial x}-\frac{2}{3}\frac{\partial}{\partial x}(\rho k)$
v	μ_{eff}	$\frac{\partial}{\partial x}\left(\mu_{\text{eff}}\frac{\partial u}{\partial r}\right)+\frac{1}{r}\frac{\partial}{\partial r}\left(r\mu_{\text{eff}}\frac{\partial v}{\partial r}\right)-2\mu_{\text{eff}}\frac{v}{r^2}-\frac{\partial p}{\partial r}-\frac{2}{3}\frac{\partial}{\partial r}(\rho k)$
w	μ_{eff}	$-\mu_{\text{eff}}\frac{w}{r^2}-\rho\frac{vw}{r}-\frac{w}{r}\frac{\partial\mu_{\text{eff}}}{\partial r}$
k	$\mu_{\text{eff}}/\sigma_k$	$G_k-\rho\varepsilon$
ε	$\mu_{\text{eff}}/\sigma_\varepsilon$	$(C_1G_k-C_2\rho\varepsilon)\varepsilon/k$

$$G_k=\mu_t\left\{2\left[\left(\frac{\partial u}{\partial x}\right)^2+\left(\frac{\partial v}{\partial r}\right)^2+\left(\frac{v}{r}\right)^2\right]+\left(\frac{\partial v}{\partial x}+\frac{\partial u}{\partial r}\right)^2+\left(\frac{\partial w}{\partial x}\right)^2+\left[r\frac{\partial}{\partial r}\left(\frac{w}{r}\right)\right]^2\right\}.$$

$\mu_{\text{eff}}=\mu_t+\mu.$

$\mu_t=C_\mu\rho k^2/\varepsilon.$

streamline curvatures, respectively. Among this kind of modification approaches, Srinivasan and Mongia[13] attempted to ensure that the sink term of dissipation rate of turbulent kinetic energy remained a positive quantity by correcting C_2 as

$$C_2=1{\cdot}92\exp(2\alpha_s Ri_s+2\alpha_c Ri_c), \tag{2}$$

where the swirl Richardson number (Ri_s) is defined as

$$Ri_s=\frac{w}{r^2}\frac{\partial}{\partial r}(rw)\Big/\left\{\left(\frac{\partial u}{\partial r}\right)^2+\left[r\frac{\partial}{\partial r}\left(\frac{w}{r}\right)\right]^2\right\}, \tag{3}$$

and the curvature Richardson number (Ri_c) is defined as

$$Ri_c=\frac{uv}{u^2+v^2}\left[\frac{1}{r}\frac{\partial}{\partial r}(ru)-\frac{\partial u}{\partial x}\right]\Big/\left[\frac{1}{r}\frac{\partial}{\partial r}(ru)+\frac{\partial v}{\partial x}\right]. \tag{4}$$

For the simulation of a strongly swirling flow, the values of α_s and α_c were suggested to be $-0{\cdot}75$ and $-2{\cdot}0$, respectively, by Srinivasan and Mongia.[13] The value of C_2 is suggested to be in the range 0·1–2·4 by Abujelala and Lilley[11] for swirling recirculating flows.

However, two problems may arise by adopting the above modification. One is that this modified k–ε model overlooks the fact that the standard k–ε model works quite successfully for predictions of simple flows, and even simple flows possess some inherent streamline curvature but with smaller magnitude than in complex flows. In recognition of this fact, a hybrid k–ε model[19] has been successfully developed and applied to the recirculating flows without swirl. Extension of this concept to the swirling recirculating flows is, therefore, expected to perform a better job than other modification methods to the k–ε models. The other problem is that the employment of the swirl Richardson number defined in equation (3) sometimes leads to a convergence difficulty in the numerical simulation of axisymmetric flows. The original work of Srinivasan and Mongia[13]

also exposed this divergence problem. Our study revealed that this was because the denominator of the swirl Richardson number might approach zero value in the neighbourhood of the axis of symmetry. Similar argument was alleged in the investigation of Bradshaw.[10] A new parameter, instead of the one defined in equation (3), accounting for the swirling effect on streamline curvature will be used in this work to avoid this singularity problem.

3. TEST PROBLEM AND NUMERICAL METHOD

3.1. Description of test problem

The experimental study of an axisymmetrical sudden-expansion flow conducted by Dellenback[20] is selected as the test problem in this work. Dellenback studied the characteristics of turbulent swirling flow through pipe expansion by using water as the working medium. The swirling motion was generated by the tangential slot entry in the upstream of the test chamber. The measurements of fluid velocity were made using a two-component laser Doppler anemometer (LDA). The diameters of inner and outer tubes were 50·8 and 98·6 mm, respectively, to achieve 0·515 expansion ratio. The test chamber was 1041·4 mm long. Details of the experimental facility and conditions are referred to Reference 20.

Three levels of swirl, low, moderate and high, were investigated in the experiment. However, Dellenback[20] reported that the asymmetric vortex was observed in the downstream flow field for the cases of low swirl level in his experiment. Similar observations have been reported in other papers.[21,22] Samimy *et al.*[22] further pointed out that there were well-organized large-scale oscillation in the low-swirl-level flows. In other words, the flow becomes a three-dimensional, time-dependent problem as the swirl level is low. For the cases of moderate and high swirl levels, the flows exhibited the steady-state and axisymmetric characteristics and the CTRZ was formed in the flow field[20] as schematically shown in Figure 1. The present interest is focused on the swirling recirculating flows with adequately strong swirl intensities usually occurring in high-performance combustors. Only the flows with moderate and high swirl levels in Dellenback's experiment will be analysed in the sequel. Accordingly, the problem to be addressed is a steady-state, two-dimensional flow.

3.2. Numerical solution procedure

Numerical simulation of the swirling flows with the k–ε turbulence models requires a simultaneous solution of the governing equations which include continuity, momentum, turbulent kinetic energy and its dissipation rate. These governing equations can be cast into a common form of axisymmetric cylindrical co-ordinates and are summarized in Table I. The empirical model constants are taken as $\sigma_k = 1{\cdot}0$ and $C_1 = 1{\cdot}44$. The other three model constants are dependent on the employed k–ε models and are summarized in Table II.

There are no significant differences between the current numerical solution procedure and the earlier one.[19] Therefore, the employed numerical solution procedure is briefly described here. The finite-volume method incorporated with the power-law scheme and the SIMPLER algorithm[23] is used to solve numerically the partial differential equations summarized in Table I. One may argue that numerical (or false) diffusion can be introduced through the discretization of the governing equations, particularly for the problem in complex flows of streamline-to-grid skewness. The use of a higher-order numerical scheme can, to a certain degree, reduce the numerical diffusion.[24,25] Nevertheless, the use of high-order numerical schemes sometimes reduces the numerical stability. This is a serious concern in the case of chemically reacting flows,[5] which will be our research interest in next step.

Table II. Empirical constants in various k–ε models

Model		C_μ	σ_ε	C_2
1	(Standard k–ε)	0·09	1·3	1·92
2	(Reference 11)	0·125	1·1949	1·5942
3	(Present work)	0·09	1·3	Equations (10) and (11)

To use the power-law scheme successfully, for the complex flows such as in the present work, care must be taken in establishing the grid mesh. It is not just the total number of grid nodes that matters, but also the distribution of grid nodes within the computational domain.[5] Distribution of grid nodes employed in this work is arranged to ensure that small regions that exert a large influence on the flow field are adequately resolved. A grid mesh composed of 50×40 (axial by radial ordinates) is used for flow field computation. Numerical tests showed that this non-uniform grid mesh yields a nearly grid-independent solution (with less than 1% change in prediction of the reattachment length as compared to that obtained with the grid mesh of 150×70). The convergence criterion adopted in computation is set so that the summation of the absolute value of the normalized residual in the entire computational domain for each dependent variable ϕ is less than 10^{-3}.

Due to the elliptic nature of the governing equations listed in Table I, boundary conditions should be specified at all the boundaries of the computational domain, including the inlet, outlet, confined wall and symmetric axis boundaries. The boundary condition at the confined wall can be realistically made using the conventional wall function treatment to bridge the no-slip wall to the fully turbulent region. For the symmetric axis, except for the radial velocity component which is itself zero, the assumption of gradient-type boundary conditon, $\partial\phi/\partial r = 0$, is made. Jones and Pascau[17] as well as Hogg and Leschziner[18] discussed the importance of the Outlet Boundary Condition (OBC) on the prediction accuracy for flows with subcritical swirl. In contrast, Nikjooy and Mongia[15] argued that the use of the fully developed specification as the OBC in their test cases (computational domain = 300 mm, swirl angle = 60°) led to satisfactory predictions since no apparent axial variations of the measured properties were observed in the upstream locations ($x > 150$ mm). Since no available measured information was provided by Dellenback,[20] the use of the measured profiles as the OBC is impossible. However, similar observations of very small axial variations for both axial and tangential velocity components, as argued in Reference 15, can be found at $x/D = 5$ in the present investigated cases. In addition, the computational domain, which is the same as the physical domain investigated by Dellenback,[20] extends to an axial distance of 10·56 diameter of the outer tube (D). The fully developed OBC is then employed in the present calculations.

Only two mean and fluctuating (axial and tangential) velocity components were measured in Dellenback's experiment.[20] Furthermore, no velocity measurements were made right at the inlet section ($x/D = 0$). In order to provide a proper specification of the mean axial and tangential velocity profiles at the inlet, the inlet profiles are obtained by linearly extrapolating the data at two consecutively neighbouring upstream sections ($x/D = -1{\cdot}0$ and $-0{\cdot}25$), which were available in the experiment, to the inlet section. The inlet values of the mean radial velocity component are assumed to be zero in the absence of better information. Due to inadequate information provided in Dellenback's experiment to calculate the turbulent kinetic energy k, the inlet profiles for k and

ε are given in the usual empirical manner:[26]

$$k_{in} = 0{\cdot}03 u_{in}^2, \tag{5}$$

$$\varepsilon_{in} = k_{in}^{1{\cdot}5}/(0{\cdot}005 D_1). \tag{6}$$

Note that, as observed from the Dellenback's measurements of axial and tangential turbulent intensities in the sections around the inlet, a high level of k such as shown in equation (5) is expected. However, Nallasamy and Chen[27] showed that the influence of the inlet boundary conditions of k and ε for the confined swirling flows in pipe expansion was appreciable only in the initial region of the flow field and became less significant in the downstream region.

4. RESULTS AND DISCUSSION

Four flow cases, which were experimentally tested by Dellenback,[20] with swirl intensities ranging from moderate to high levels, are selected as the comparison basis for this work. Note that, according to the experimental observations, all the four selected swirl flows possessed CTRZ and CRZ in their flow fields as demonstrated schematically in Figure 1.

4.1. Development of hybrid modification to k–ε model

In order to avoid the previously stated singularity problem in the use of the swirl Richardson number defined by equation (3), the gradient Richardson number, which represents the square of the ratio of Brunt–Väisälä frequency to typical turbulent frequency (or the ratio of typical body force to typical inertial force) and is expressed by[10]

$$Ri_g = \left(\frac{\text{Brunt Väisälä frequency}}{\text{typical turbulent frequency}} \right)^2 = \frac{\omega_{BV}^2}{\omega_t^2}, \tag{7}$$

where the Brunt–Väisälä frequency, ω_{BV}, and the turbulent frequency, ω_t, are given, respectively, by

$$\omega_{BV} = \left[2 \frac{w}{r^2} \frac{\partial}{\partial r} (rw) \right]^{0{\cdot}5} \tag{8}$$

and

$$\omega_t = \left[\left(\frac{\partial u}{\partial r} \right)^2 + \left(\frac{\partial w}{\partial r} \right)^2 \right]^{0{\cdot}5}, \tag{9}$$

is introduced into the modification formalism, instead, to describe the swirl effects. However, since the order of magnitude of Ri_g may reach as high as 10^3 for the test cases, a normalized substitution, $1/(Ri_g + 1)$, is employed in the present modelling work. Figures 2(a) and 2(b) demonstrate stereographically a typical distribution of $1/(Ri_g + 1)$ for the test case of $Re = 30\,000$ and $S = 0{\cdot}98$ in the inlet region and the overall flow field, respectively. As revealed by Figure 2, high values of $1/(Ri_g + 1)$ are primarily distributed along the shear layers: one is in the intermixing zone between the CRZ and the CTRZ (near the inlet), and the other is in the near-wall regions. Following the definition of equation (7), the Ri_g values can never be negative. Nevertheless, a check from Figures 2(a) and 2(b) shows that some values of $1/(Ri_g + 1)$ distributed in the near-wall regions exceed unity. This implies that some Ri_g's become negative, which are physically meaningless as to be interpretated in terms of the Brunt–Väisälä frequency, in the near-wall regions. In addition, based on a basic criteria adopted in this work, the modifications need not be made in the regions where the flow behaviours can be satisfactorily predicted using the standard

k–ε model. The shear layer in the near-wall regions, which are usually categorized as a simple flow, should not be subject to modification. As a result, a threshold value for ω_{BV}^2 has to be set in the model to prevent the occurrence of the above undesirable problem.

Figure 3 demonstrates stereographically a typical distribution of Ri_c for the test case of $Re = 30\,000$ and $S = 0{\cdot}98$ in the overall flow field. Obviously, the high recirculating streamline curvatures (Ri_c) are distributed only around the inlet. Also, the maximum value of Ri_c may be one order of magnitude larger than that of the non-swirling case investigated previously.[19] According

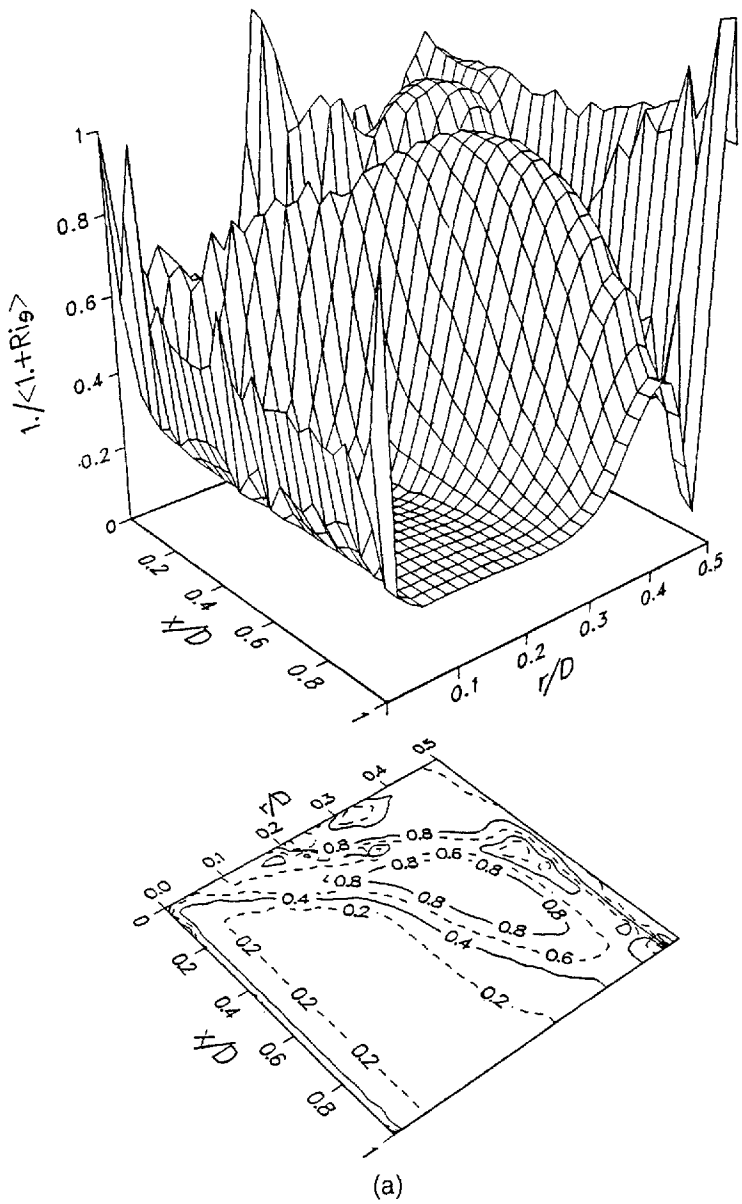

Figure 2. Typical distributions of $1/(Ri_g+1)$ in (a) inlet region and (b) overall flow field

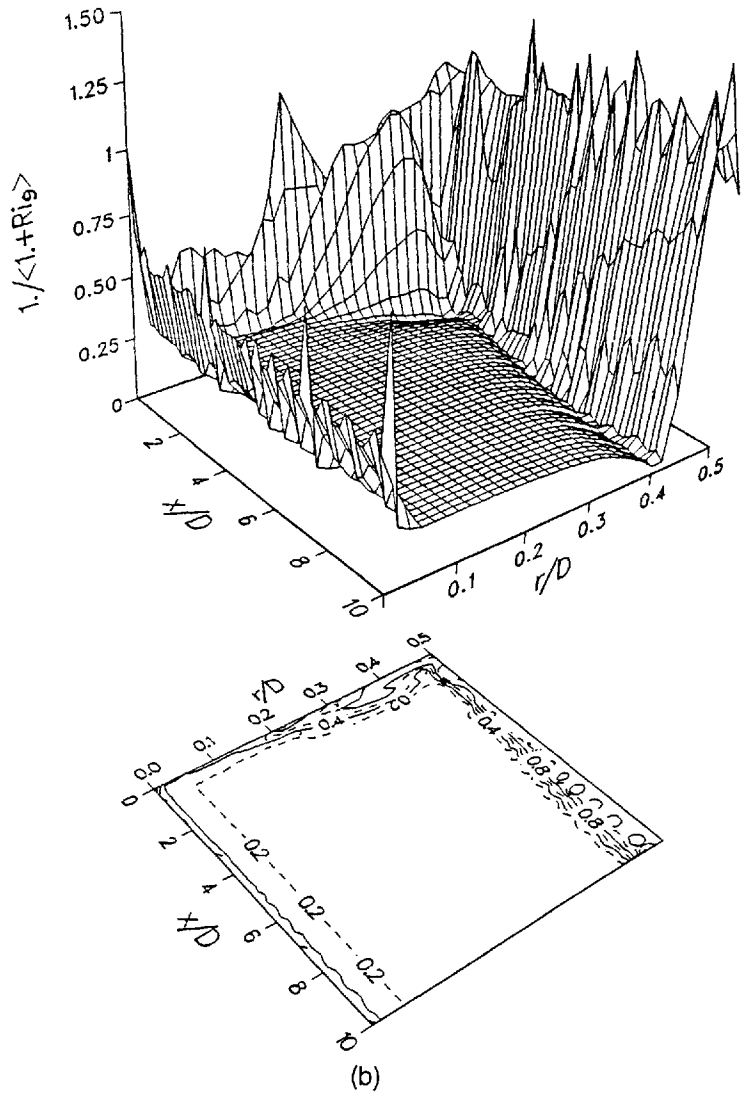

Figure 2. (Continued)

to the observations made from Figures 2 and 3, the following inferences can be drawn: (1) significant swirling anisotropic effect is distributed mainly in the shear layer between the CRZ and the CTRZ; (2) there exist both swirling and recirculating anisotropic effects in the CRZ, while there exists only swirling anisotropic effect in the CTRZ; and (3) the modification to swirling anisotropic effect needs not to be made for the shear layer in the near-wall regions.

Based on these three general inferences, a number of attempts using the flow cases with swirl intensities from moderate to high levels ($S = 0{\cdot}6 - 1{\cdot}23$) have been made to find the best comparison of the model predictions with the measurements of Dellenback.[20] A hybrid modification to

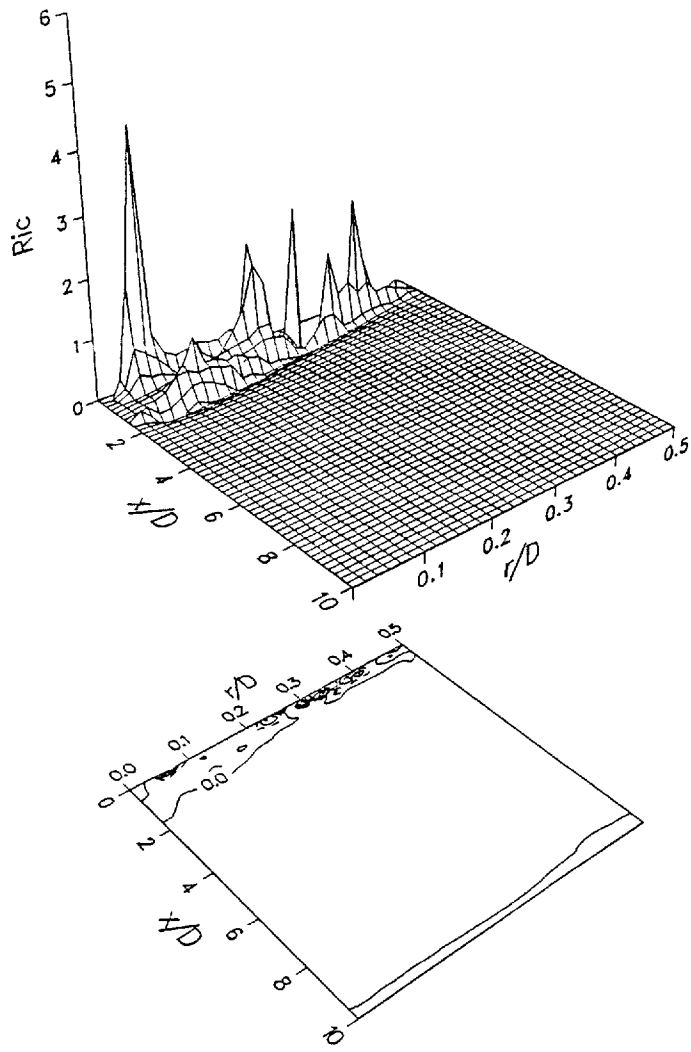

Figure 3. Typical distribution of Ri_c in overall flow field

C_2, instead of equation (1), is then suggested as follows:

$$C_2^* = 1{\cdot}92 \exp(4Ri_c) \quad \text{for } Ri_c \geq 0{\cdot}2, \tag{10a}$$

$$C_2^* = 1{\cdot}92 \quad \text{for } Ri_c < 0{\cdot}2 \tag{10b}$$

and

$$C_2 = C_2^* \exp\left(\frac{S/3 - 1{\cdot}4}{Ri_g + 1}\right) \quad \text{for } \left(\frac{1}{Ri_g + 1} \geq 0{\cdot}3 \quad \text{and } \omega_{BV}^2 \geq 0{\cdot}5\right) \quad \text{or} \quad Ri_c \geq 0{\cdot}2, \tag{11a}$$

$$C_2 = C_2^* \text{ for } \left(\frac{1}{Ri_g + 1} < 0{\cdot}3 \quad \text{or } \omega_{BV}^2 < 0{\cdot}5\right) \quad \text{and} \quad Ri_c < 0{\cdot}2. \tag{11b}$$

Note that the C_2 modification formalism in terms of Ri_c, equation (10), is different from the previous work developed for the non-swirling case.[19] The main concern of the previous Ri_c modification for the non-swirling flows was placed on the reduction of the predicted turbulent kinetic energy in the CRZ through decreasing the sink term in the ε equation (see Table I). In contrast, experimental observations[10, 20] revealed that the turbulence intensities in the CRZ are strengthened owing to the free-vortex effects for the flows with moderate and high swirl levels. Furthermore, the present design of C_2 modification in terms of Ri_g, equation (11), would aggravate the increment need of turbulent kinetic energy in the CRZ. In order to meet this need, the present model proposes an opposite way of C_2 modification due to Ri_c consideration compared to the previous modification formalism for the non-swirling case,[19] in order to increase the predicted turbulent kinetic energy in the CRZ. One thing shoud be noted that the application of equations (10) and (11) to non-swirling flows or to flows with low swirl levels is definitely unsuitable.

It is obvious that there remains a gap between the present work (flows with moderate and high swirl levels) and our previous work (non-swirling flow), i.e. flows with low swirl levels, which have not been studied yet. More research efforts including theoretical and experimental studies for flows with low swirl levels (characterized by unsteady-state, three-dimensional nature) are required to construct a universal modification formalism accounting for the anisotropic effects due to recirculating streamline curvature.

4.2. *Validation of hybrid k- ε model*

Three turbulence models, including the standard k–ε model (Model 1), the modified k–ε model proposed by Abujelala and Lilley[11] (Model 2), and the present hybrid k ε model (Model 3) are tested in this work. The differences among these three models are listed in Table II. The measurements of Dellenback[20] were made in the whole radial section (from $r/D = -0{\cdot}5$ to $0{\cdot}5$) at each investigated axial station although the tested flows were taken as axisymmetric cases. A detailed check of the measured data in the upper- and lower-half sections individually for the selected flow cases shows a satisfactory axisymmetric feature.

Case 1: Moderate swirl level ($S = 0{\cdot}6$, $Re = 30\,000$). The predicted profiles of the mean axial velocity component at various axial stations obtained with these three turbulence models are presented in Figure 4 and compared with the measured data. As stated before, the use of the assumed inlet profiles of v, k and ε may bring in some prediction errors in the very near inlet region. However, this kind of errors can be overlooked if we focus our attention on the downstream flow field far enough from the inlet (say, $x/D > 0{\cdot}5$). Clearly, the standard k ε model (Model 1) gives the maximum underprediction of the length of CTRZ, while the other two models yield comparatively better predictions of the length of CTRZ. However, the modified k–ε model proposed by Abujelala and Lilley[11] (Model 2) yields poor predictions of the axial velocity component in the upstream regions compared to Models 1 and 3. The hybrid k–ε model (Model 3) has closer performance as that of Model 1 in the upstream regions and can improve, to certain extent, the prediction accuracy in the downstream regions compared to Model 1.

The predicted profiles of the mean tangential velocity component at various axial stations obtained with the three turbulence models are presented in Figure 5 and compared with the measured data. The comparison shows that Model 2 gives the most satisfactory predictions while Model 1 gives the worst predictions among these three models. However, the adoption of hybrid modification concept in the k–ε model (Model 3) can improve the prediction capability as made by the standard one (Model 1).

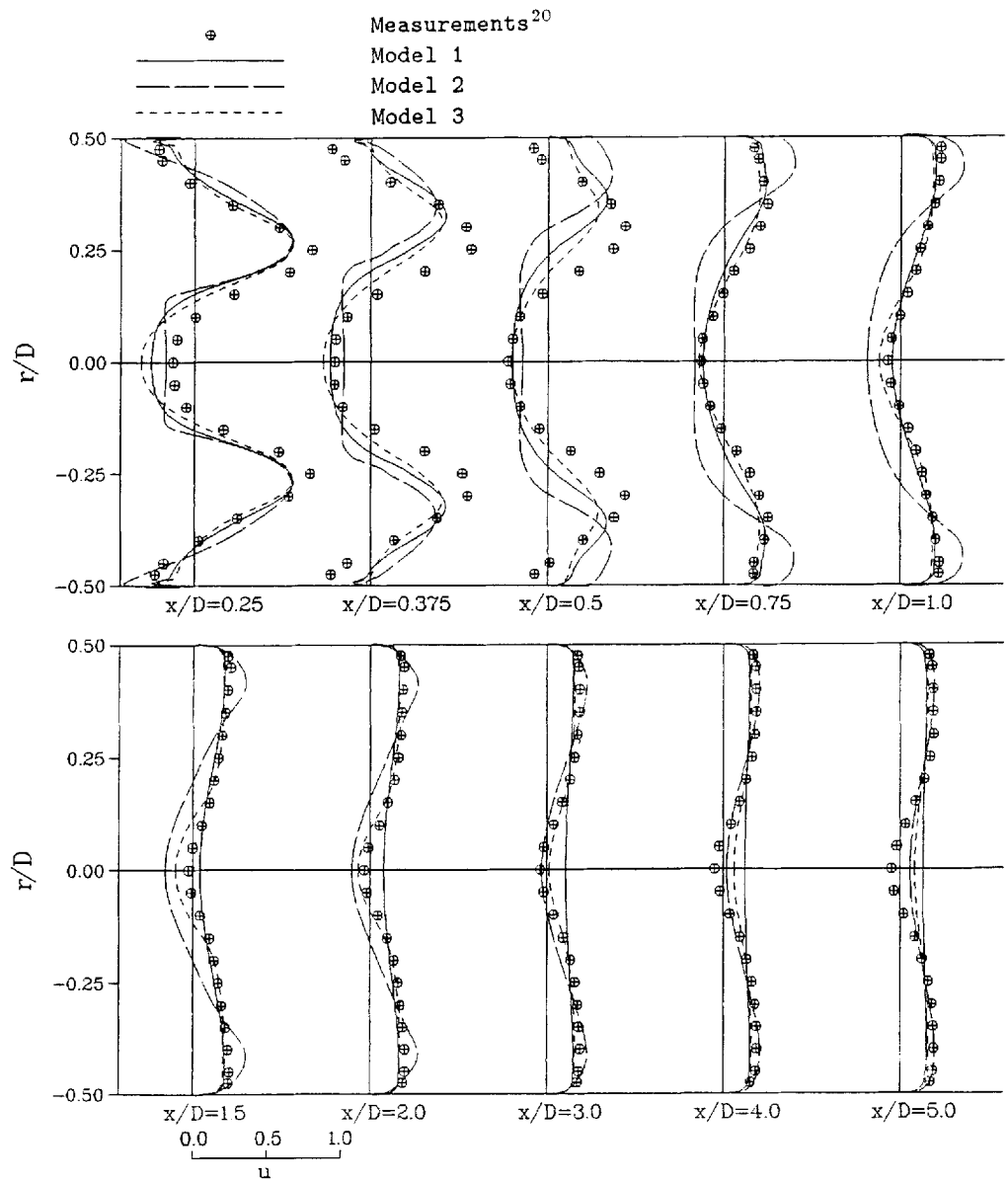

Figure 4. Comparison of the measured and the predicted mean axial velocity components for Case 1 ($S = 0{\cdot}6$, $Re = 30\,000$)

One important transport property, the eddy viscosity (μ_t), which is determined by the calculated values of k and ε, as defined in Table I, can greatly affect the diffusion coefficients in turbulent transport processes such as momentum, heat and mass transfers. The contour maps of turbulent viscosity obtained with Models 1 and 3 are plotted in Figures 6 and 7, respectively. A comparison between Figure 6 and Figure 7 shows that the predicted μ_t values obtained with Model 1 are generally greater than those obtained with Model 3 in the upstream flow field. This

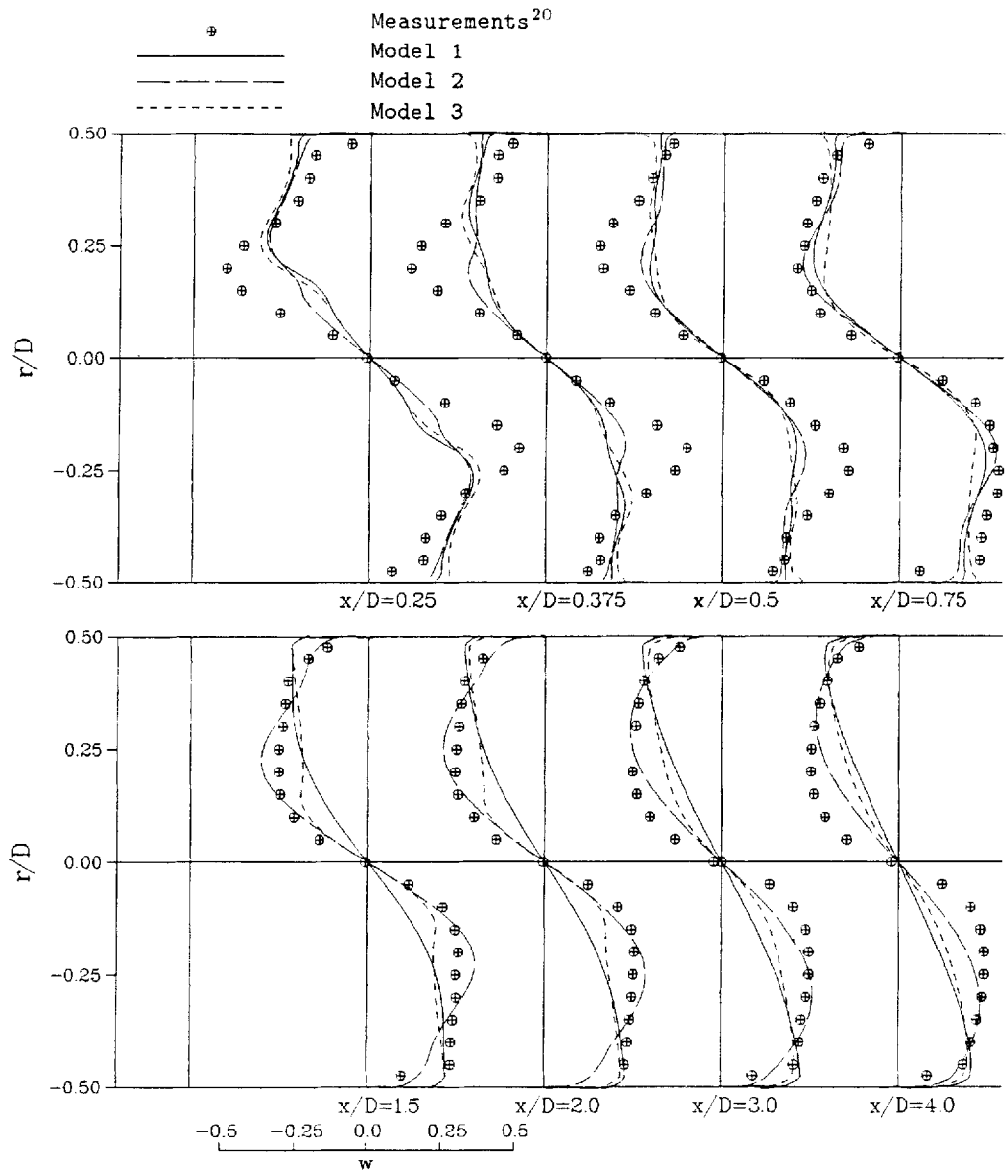

Figure 5. Comparison of the measured and the predicted mean tangential velocity components for Case 1 ($S=0{\cdot}6$, $Re=30\,000$)

may explain why the predicted u profiles using Model 1 reach their fully developed flow pattern in a shorter distance as compared to that using Model 3 (see Figure 4).

Case 2: High swirl level ($S=0{\cdot}98$, $Re=30\,000$). Figures 8 and 9 show comparisons of the predicted (using the three investigated turbulence models) and the measured mean axial and tangential velocity components, respectively, for a high-swirl-level case. Comparisons of the measurements and the predictions reveal that the standard k–ε model (Model 1) is unable to

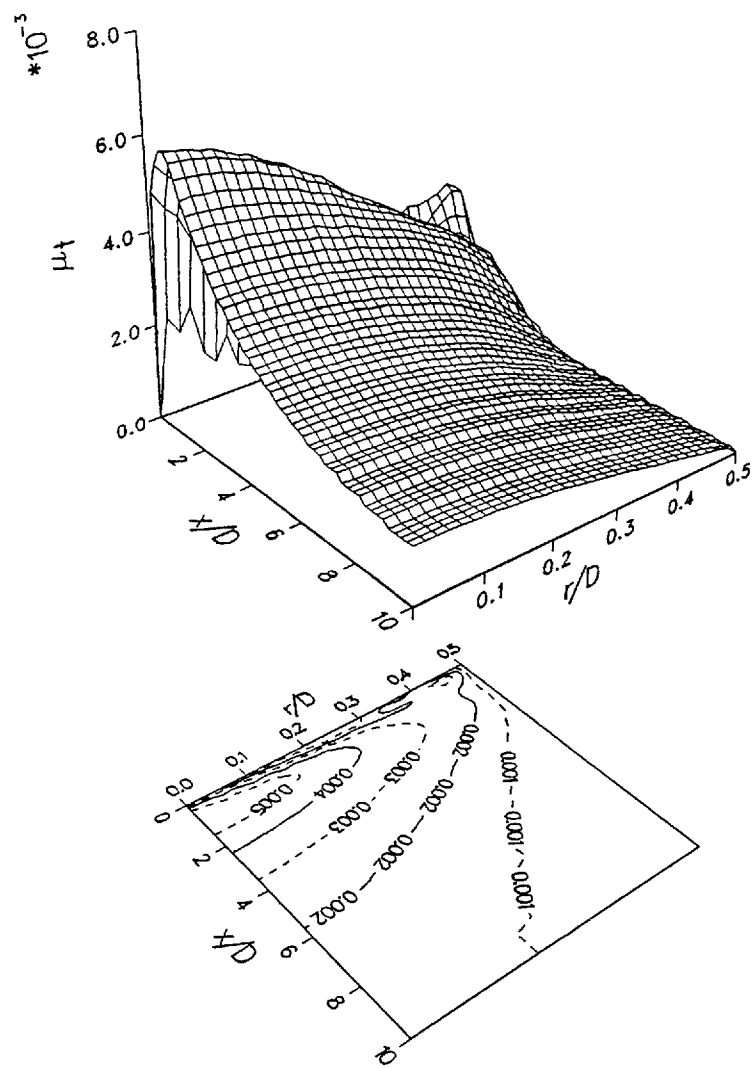

Figure 6. Contour map of the predicted μ_t for Case 1 ($S=0{\cdot}6$, $Re=30\,000$) using the standard k–ε model

predict the principal features accurately. For instance, Model 1 gives a very poor prediction of the CTRZ size (see Figure 8) and overpredicts significantly the size of the forced-vortex flow region (see Figure 9). For Model 2, trends similar to those already described above for the moderate-swirl-level case are observed. In contrast, the developed hybrid model (Model 3) can yield pretty satisfactory prediction of the CTRZ size and improve the prediction capability for the profiles of the tangential velocity component. Sultanian[14] also investigated numerically the same swirling flow case using the ASM turbulence model. However, even with this high-order closure model, Sultanian's work did not yield the flowfield predictions as good as those using Model 3, particularly in the CTRZ region.

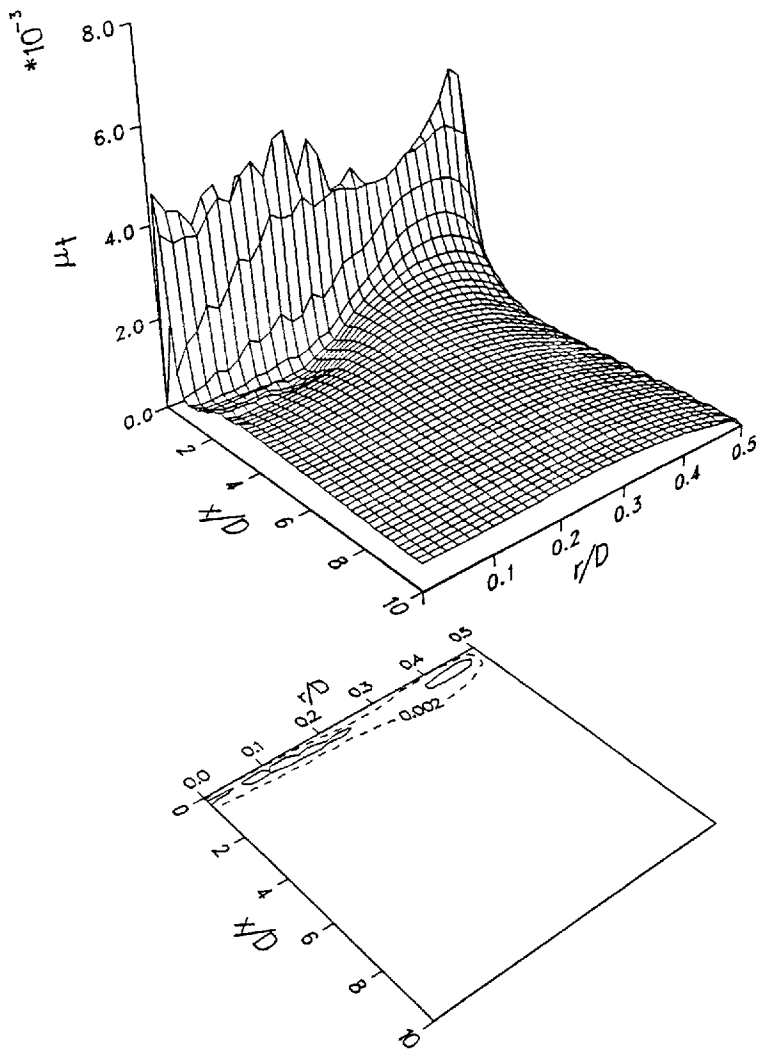

Figure 7. Contour map of the predicted μ_t for Case 1 ($S=0{\cdot}6$, $Re=30\,000$) using the hybrid k–ε model

Two more cases with higher swirl levels, which were not studied in the numerical investigation conducted by Sultanian,[14] are tested in the sequel to examine the generality and applicability of the developed hybrid model.

Case 3: High swirl level ($S=1{\cdot}16$, $Re=60\,000$). Figures 10 and 11 show comparisons of the predicted (using the three investigated turbulence models) and the measured mean axial and tangential velocity components, respectively. Similar conclusions as made for Case 2 can be drawn from these comparison results. In other words, the developed hybrid k–ε model gives the most satisfactory predictions of the axial and the tangential velocity components among the three investigated turbulence models.

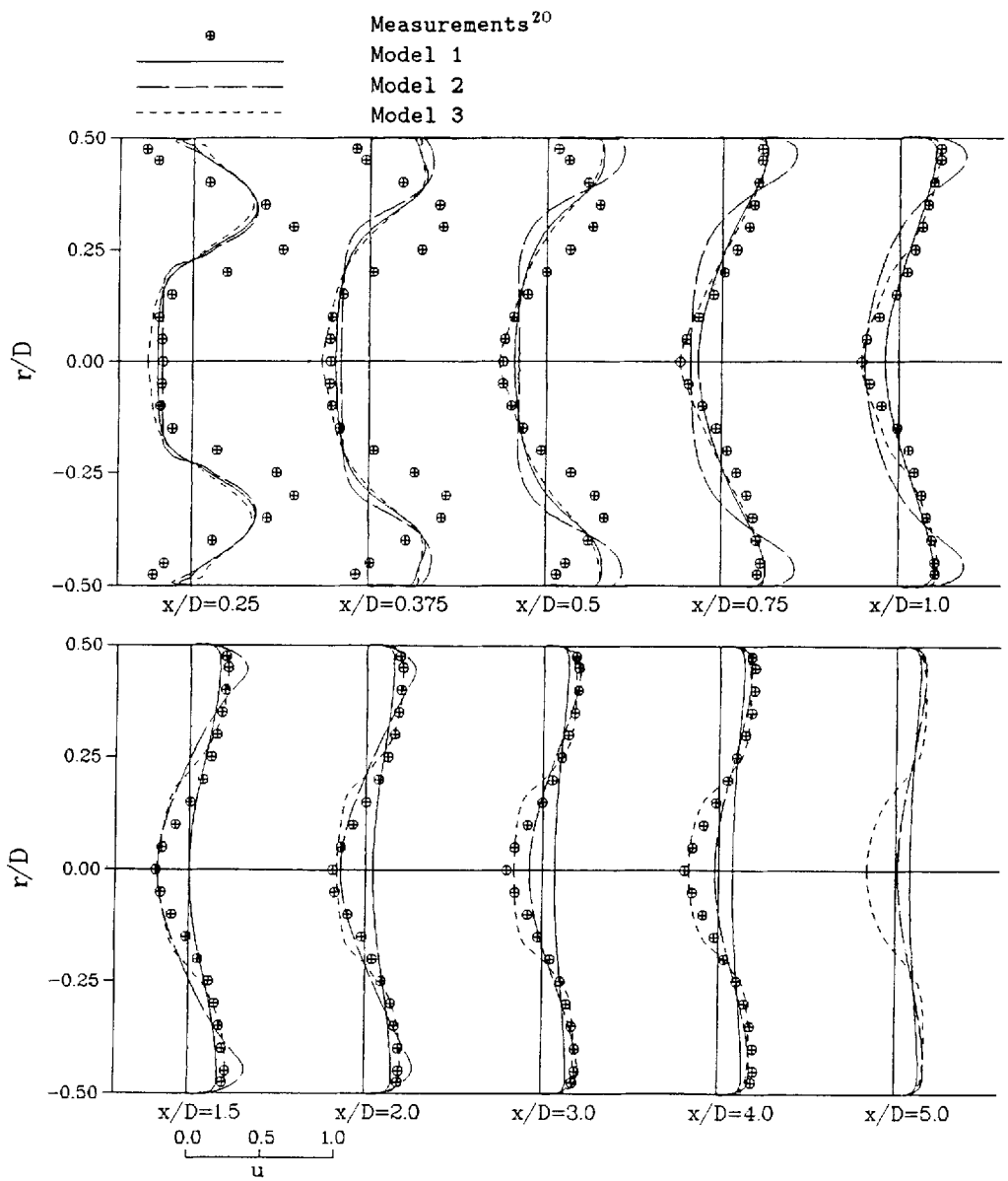

Figure 8. Comparison of the measured and the predicted mean axial velocity components for Case 2 ($S = 0{\cdot}98$, $Re = 30\,000$)

Case 4: High swirl level ($S = 1{\cdot}23$, $Re = 100\,000$). Experimental results[20] showed that, as the swirl number was increased to 1·23, the flow with apparent off-axis recirculation (see Figure 12) was observed, while the on-axis recirculation was observed for flows with relatively smaller swirl numbers, such as Cases 1 and 2. Also, the on-axis tangential velocity gradient becomes steep throughout the downstream regions, as shown in Figure 13. These two features cannot be wholly discerned from the experimental results of Case 3, with $S = 1{\cdot}16$, presented in Figures 10 and 11,

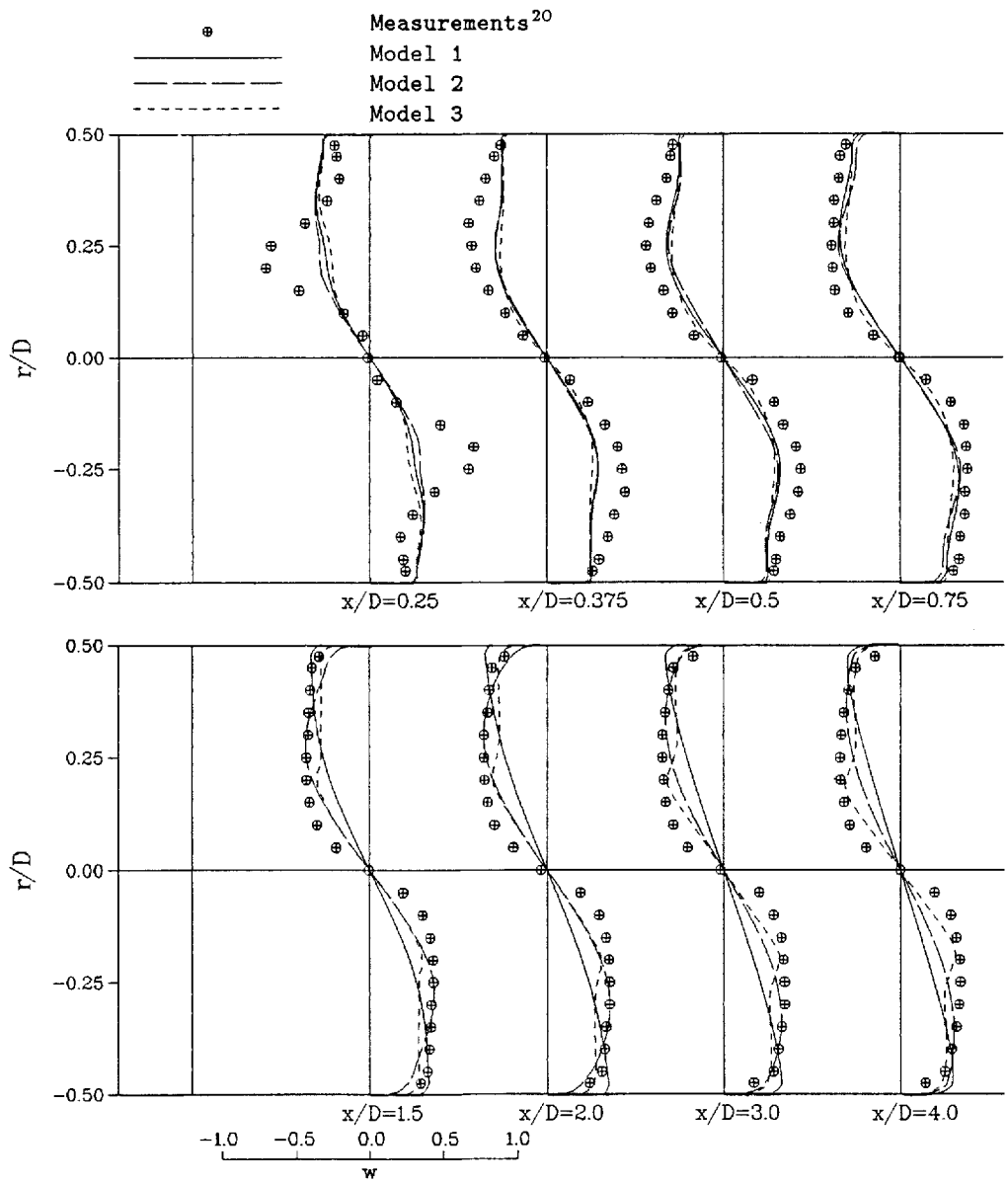

Figure 9. Comparison of the measured and the predicted mean tangential velocity components for Case 2 ($S=0{\cdot}98$, $Re=30\,000$)

but the trends towards the off-axis CTRZ and increasing tangential velocity gradients at the axis seem to be present. It is noted that the model simulation of the swirling flows with the off-axis CTRZ is seldom discussed in open literature.

Comparisons of the three predicted and the measured mean axial and tangential velocity components are presented in Figures 12 and 13, respectively. As observed from Figure 12, none of the three investigated models can simulate accurately the off-axis tendency of the CTRZ. Again,

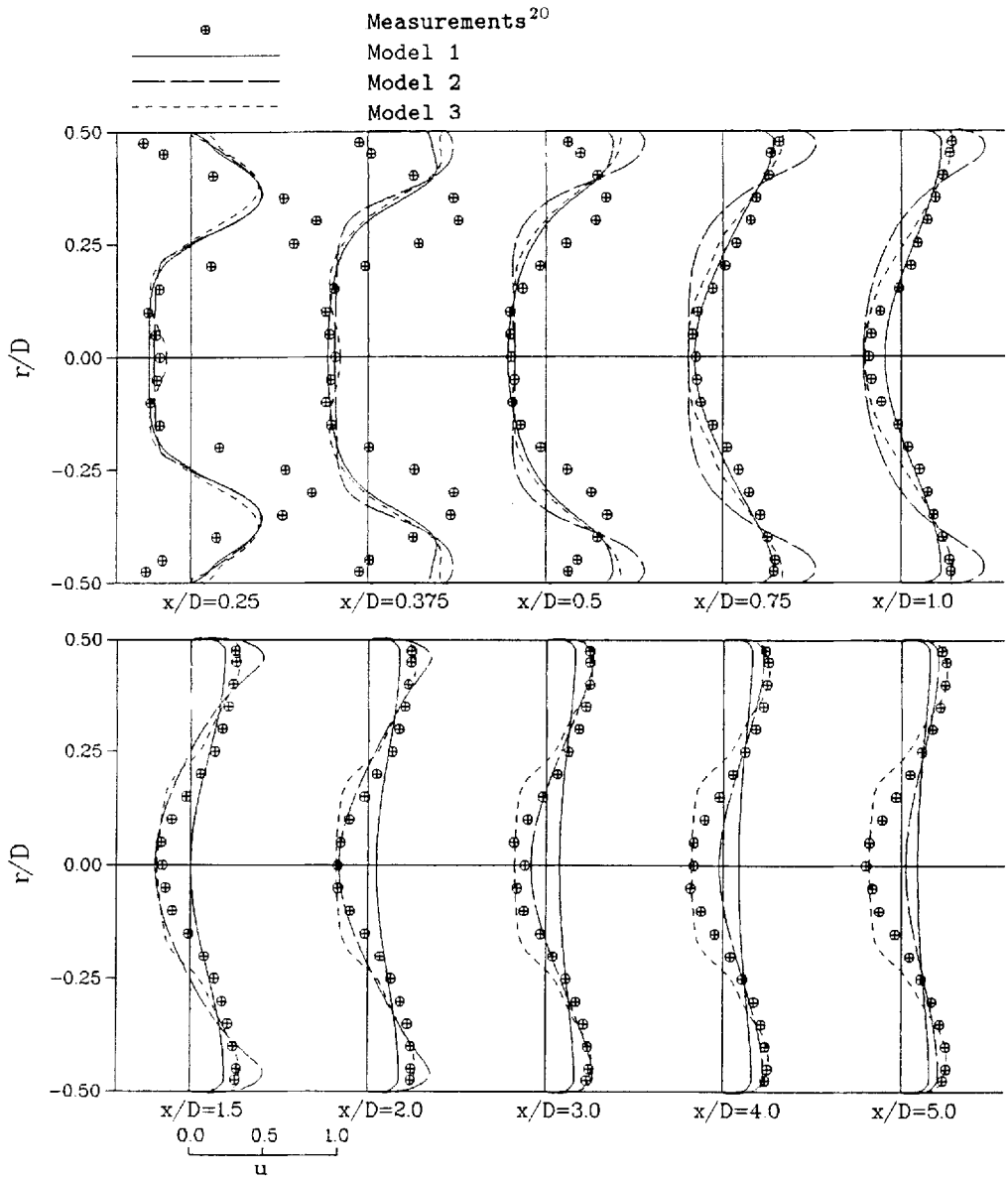

Figure 10. Comparison of the measured and the predicted mean axial velocity components for Case 3 ($S=1{\cdot}16$, $Re=60\,000$)

the standard k–ε model gives the most unsatisfactory predictions, while the developed hybrid k–ε model provides comparatively more improvements of the predictions among the three investigated models in the study.

As far as computation effort is concerned, the price to be paid for using the developed hybrid k–ε model is an approximately 100% more CPU time required to attain the same convergent level in comparison with that required by the standard k–ε model, while the employment of the

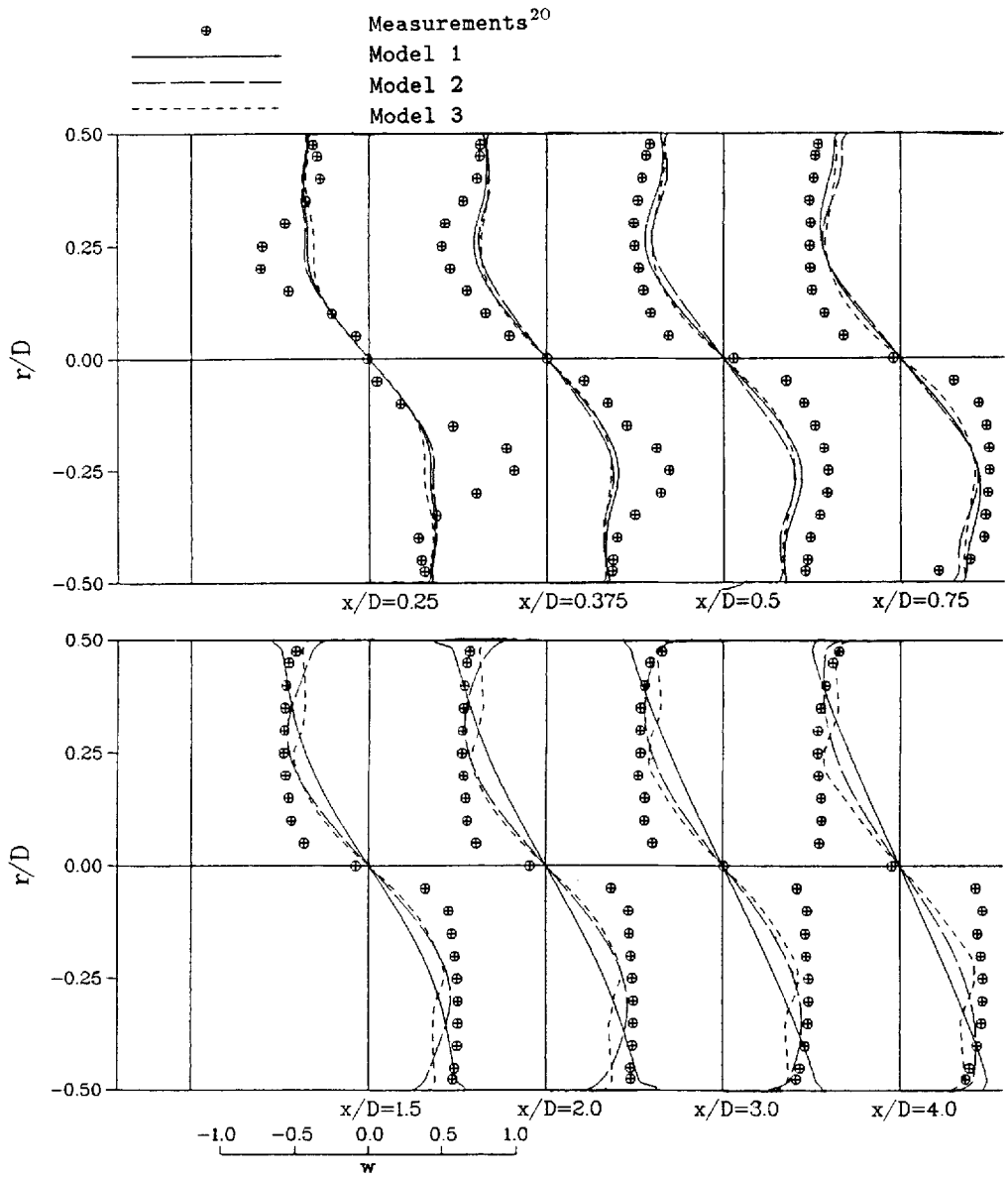

Figure 11. Comparison of the measured and the predicted mean tangential velocity components for Case 3 ($S = 1{\cdot}16$, $Re = 60\,000$)

modified k–ε model proposed by Abujelala and Lilley[11] requires approximately the same CPU time as does the standard k–ε model. It was reported by Sultanian[14] that the numerical simulations of the moderate-swirl case (Case 1) and the high-swirl case (Case 2) using the ASM required about 16 times and 30 times, respectively, as much CPU time as that required by the standard k–ε model. Note that the reported improvements of the flowfield predictions using the ASM in Sultanian's work[14] were not as applausive as those using the developed hybrid k–ε model in this work, particularly for the predictions of CTRZ size.

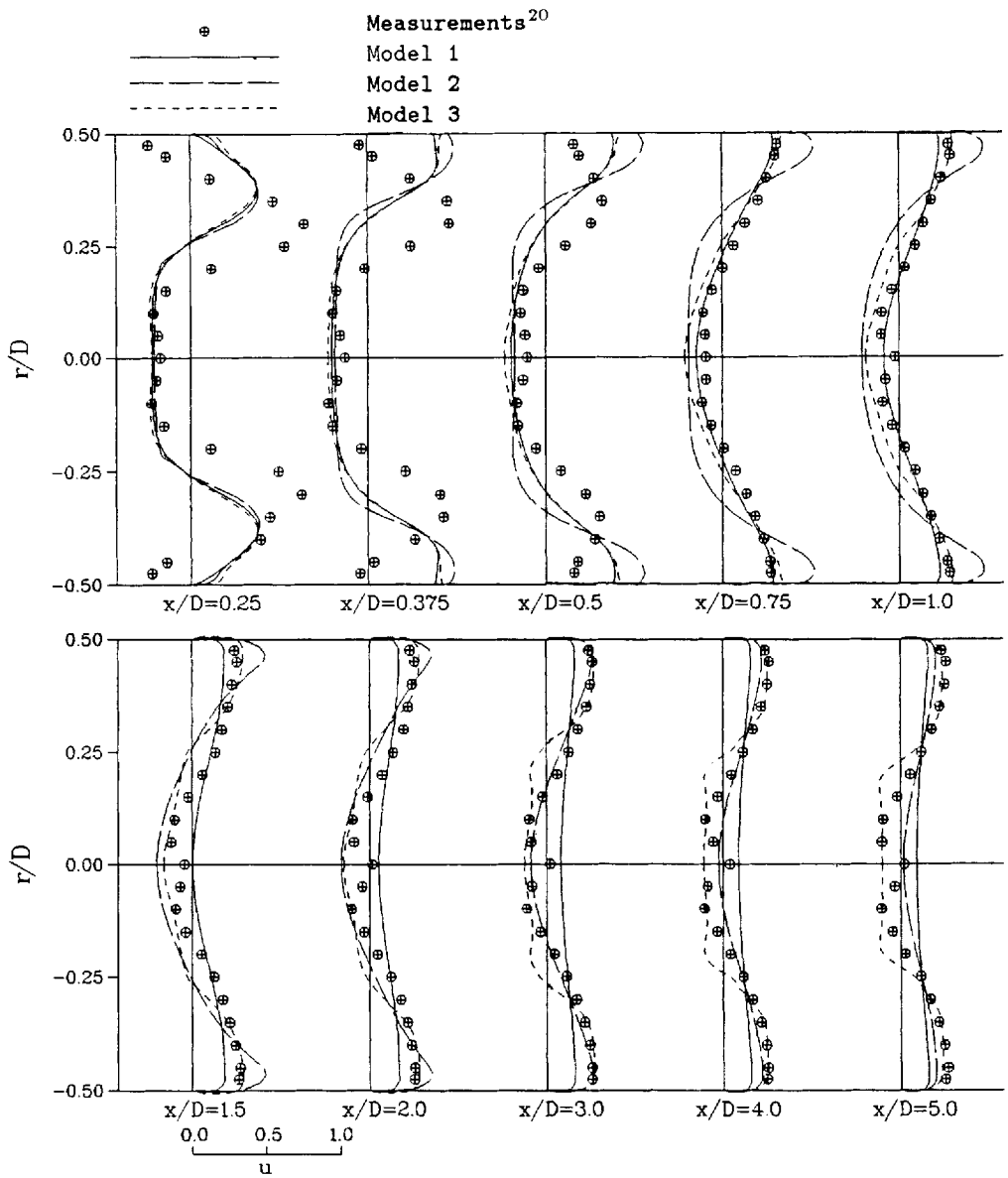

Figure 12. Comparison of the measured and the predicted mean axial velocity components for Case 4 ($S=1{\cdot}23$, $Re=100\,000$)

5. CONCLUSIONS

Based on the concept that, for regions in which the streamline curvature is small, the modification of streamline curvature effects should not be made for simulation, a hybrid k–ε model, in terms of the curvature Richardson number, the gradient Richardson number and the Brunt–Väisälä frequency, is developed and expressed in terms of equations (10) and (11). The developed hybrid model is examined with swirling recirculating flows under moderate to strong swirl intensities

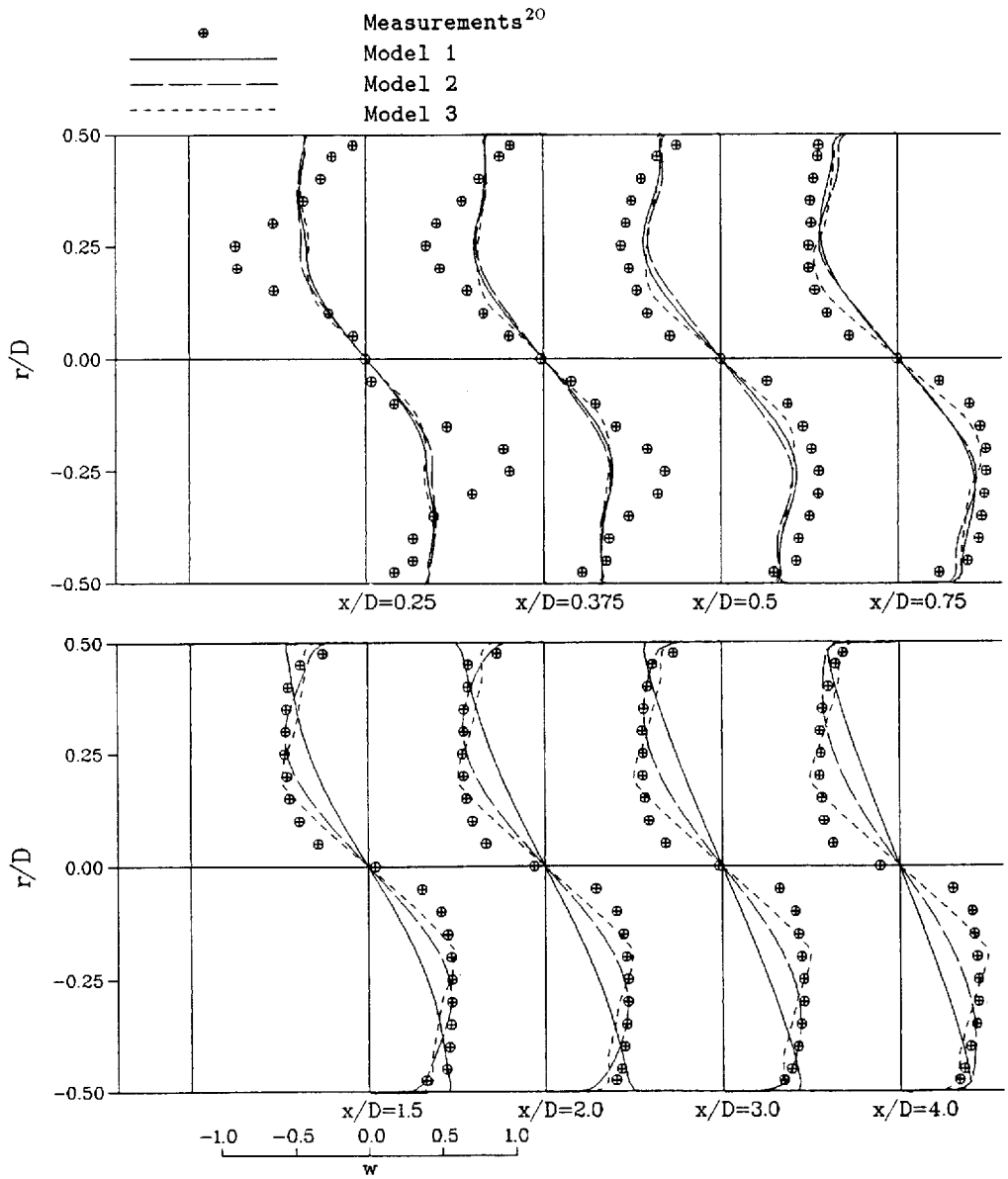

Figure 13. Comparison of the measured and the predicted mean tangential velocity components for Case 4 ($S = 1{\cdot}23$, $Re = 100\,000$)

and compared with the corresponding experimental results of Dellenback.[20] Comparisons show that this hybrid model can yield the location and size of CTRZ fairly well and improve, to some extent, the prediction accuracy of the size of forced-vortex flow region in comparison with the standard k–ε model and the modified k–ε model proposed by Abujelala and Lilley.[11]

However, the application of this hybrid model to calculations of much highly swirling flows ($S \geq 1{\cdot}23$) does not capture some flow features such as the off-axis tendency of the CTRZ and yields poor predictions of the mean tangential velocity component. For these much highly

anisotropic flows, the RSM may be the only choice to try although the computational effort and the complexity are much increased. It should be emphasized that the developed hybrid k–ε model is able to provide reasonably accurate and yet economical calculations for the tested cases with the swirl levels ranging from 0·6 to 1·23.

APPENDIX I: NOMENCLATURE

ASM	algebraic stress models
C_1, C_2, C_μ	constants of turbulence model
CRZ	corner recirculation zone
CTRZ	central toroidal recirculation zone
D	diameter of outer tube
D_1	diameter of inner tube
G	production term
k	turbulent kinetic energy
p	pressure
Re	Reynolds number
Ri_c	curvature Richardson number
Ri_g	gradient Richardson number
Ri_s	swirl Richardson number
RSM	Reynolds stress models
r	radial co-ordinate
S	source term, swirl number
u	mean axial velocity component
v	mean radial velocity component
w	mean tangential velocity component
x	axial co-ordinate

Greek letters

Γ	diffusion coefficient
ε	dissipation rate of turbulent kinetic energy
μ, μ_t	molecular and eddy viscosity, respectively
ω_{BV}	Brunt–Väisälä frequency
ω_t	typical turbulence frequency
ρ	density
σ	turbulent constant correlated with diffusion coefficient
ϕ	dependent variable

Subscript

eff	effective value
k	turbulent kinetic energy
ε	dissipation rate of turbulent kinetic energy

REFERENCES

1. D. G. Lilley, 'Swirl flows in combustion: a review', *AIAA J.*, **15**, 1063–1078 (1977).
2. A. K. Gupta, D. G. Lilley and N. Syred, *Swirl Flows*, Abacus Press, Kent, Ohio, 1984.

3. D. G. Sloan, P. J. Smith and L. D. Smoot, 'Modeling of swirl in turbulent flow systems', *Prog. Energy Combust. Sci.*, **12**, 163–250 (1986).
4. M. Nallasamy, 'Turbulence models and their applications to the prediction of internal flows: a review', *Comput. Fluids*, **3**, 151–194 (1987).
5. G. J. Sturgess and S. A. Syed, 'Calculation of confined swirling flows', *Int. J. Turbo Jet Engines*, **7**, 103–121 (1990).
6. C. P. Chen, 'Calculation of confined swirling jets', *Commun. Appl. Numer. Methods*, **2**, 333–338 (1986).
7. M. Nallasamy, 'Computation of confined turbulent coaxial jet flows', *J. Propulsion Power*, **3**, 263–268 (1987).
8. S. C. Favaloro, A. S. Nejad and S. A. Ahmed, 'Experimental and computational investigation of isothermal swirling flow in an axisymmetric dump combustor', *J. Propulsion Power*, **7**, 348–356 (1991).
9. P. Koutmos and J. J. McGuirk, 'Isothermal modeling of gas turbine combustors: computational study', *J. Propulsion Power*, **7**, 1064–1091 (1991).
10. P. Bradshaw, 'Effects of streamline curvature on turbulent flows', *AGARDograph Report No. 169*, 1973.
11. M. T. Abujelala and D. G. Lilley, 'Limitations and empirical extensions of the k–ε model as applied to turbulent confined swirling flow', *Chem. Eng. Commun.*, **31**, 223–236 (1984).
12. J. M. Khodadadi and N. S. Vlachos, 'Effects of turbulence model constants on computation of confined swirling flows', *AIAA J.*, **28**, 750–752 (1990).
13. R. Srinivasan and H. C. Mongia, 'Numerical computation of swirling recirculating flows: final report', *NASA CR-165196*, 1980.
14. B. K. Sultanian, 'Numerical modeling of turbulent swirling flow downstream of an abrupt pipe expansion', *Ph.D. Thesis*, Arizona State University, Tempe, Arizona, 1984.
15. M. Nikjooy and H. C. Mongia, 'A second-order modeling study of confined swirling flow', *Int. J. Heat Fluid Flow*, **12**, 12–19 (1991).
16. S. Fu, P. G. Huang, B. E. Launder and M. A. Leschziner, 'A comparison of algebraic and differential second-moment closures for axisymmetric turbulent shear flows with and without swirl', *J. Fluids Eng., Trans. ASME*, **110**, 216–221 (1988).
17. W. P. Jones and A. Pascau, 'Calculation of confined swirling flows with a second moment closure', *J. Fluids Eng., Trans. ASME*, **111**, 248–255 (1989).
18. S. Hogg and M. A. Leschziner, 'Computation of highly swirling confined flow with a Reynolds stress turbulence model', *AIAA J.*, **27**, 57–63 (1989).
19. K. C. Chang, C. S. Chen and C. I. Uang, 'A hybrid k–ε turbulence model for recirculating flow', *Int. j. numer. methods fluids*, **12**, 369–382 (1991).
20. P. A. Dellenback, 'Heat transfer and velocity measurements in turbulent swirling flow through an abrupt axisymmetric expansion', *Ph.D. Thesis*, Arizona State University, Tempe, Arizona, 1986.
21. A. S. Nejad, S. P. Vanka, S. C. Favaloro, M. Samimy and C. Langenfeld, 'Application of laser velocimetry for characterization of confined swirling flow', *J. Eng. Gas Turbines Power, Trans. ASME*, **111**, 36–45 (1989).
22. M. Samimy, A. S. Nejad, C. A. Langenfeld and S. C. Favaloro, 'Nonaxisymmetric instabilities in a dump combustor with a swirling inlet flow', *J. Propulsion Power*, **6**, 78–84 (1990).
23. S. V. Patankar, *Numerical Heat Transfer and Fluid Flow*, McGraw-Hill, New York, 1980.
24. R. A. Beier, J. de Ris and H. R. Baum, 'Accuracy of finite-difference methods in recirculating flows', *Numer. Heat Transfer*, **6**, 283–308 (1983).
25. I. P. Castro and J. M. Jones, 'Studies in numerical computations of recirculating flows', *Int. j. numer. methods fluids*, **7**, 793–823 (1987).
26. D. G. Lilley and D. L. Rhode, 'STARPIC: a computer code for swirling turbulent axisymmetric recirculating flows in practical isothermal combustor geometries', *NASA CR-3442*, 1982.
27. M. Nallasamy and C. P. Chen, 'Studies on effects of boundary conditions in confined turbulent flow predictions', *NASA CR-3929*, 1985.